Light propagation through anisotropic turbulence

Italo Toselli,[1,*] Brij Agrawal,[1,3] and Sergio Restaino[2,4]

[1]*Mechanical and Astronautical Engineering Department, Naval Postgraduate School, Monterey, California 93943, USA*
[2]*Remote Sensing Division, NRL Code 7216, 3550 Aberdeen SE, Albuquerque, New Mexico 87117, USA*
[3]*e-mail: agrawal@nps.edu*
[4]*e-mail: sergio.restaino@gmail.com*
**Corresponding author: itoselli@nps.edu*

Received August 19, 2010; revised November 22, 2010; accepted January 3, 2011;
posted January 19, 2011 (Doc. ID 133591); published March 1, 2011

A wealth of experimental data has shown that atmospheric turbulence can be anisotropic; in this case, a Kolmogorov spectrum does not describe well the atmospheric turbulence statistics. In this paper, we show a quantitative analysis of anisotropic turbulence by using a non-Kolmogorov power spectrum with an anisotropic coefficient. The spectrum we use does not include the inner and outer scales, it is valid only inside the inertial subrange, and it has a power-law slope that can be different from a Kolmogorov one. Using this power spectrum, in the weak turbulence condition, we analyze the impact of the power-law variations α on the long-term beam spread and scintillation index for several anisotropic coefficient values ς. We consider only horizontal propagation across the turbulence cells, assuming circular symmetry is maintained on the orthogonal plane to the propagation direction. We conclude that the anisotropic coefficient influences both the long-term beam spread and the scintillation index by the factor $\varsigma^{2-\alpha}$.

OCIS codes: 010.0010, 010.1300, 010.1330.

1. INTRODUCTION

The atmosphere's statistical behavior does not always follow the Kolmogorov power spectrum density model; rather it follows different power laws [1]. Several experimental data and measurements indicate that the turbulence in the upper troposphere and stratosphere, or along nonhomogeneous path, deviates from predictions of the Kolmogorov model [2–6]. Other experiments showed that atmospheric turbulence in maritime environments can assume a different statistical behavior with respect to Kolmogorov [7–13]. In addition, anisotropy in stratospheric turbulent inhomogeneities has been experimentally investigated [14–17], and laboratory results have shown that turbulence can be anisotropic. These studies cast doubt on the correctness of the conventional assumption of isotropic turbulence through the entire atmosphere. Also, researchers have collected data at high altitudes that indicate the existence of anisotropic turbulence and non-Kolmogorov behavior [18].

Kon [19] qualitatively analyzed the effect of the anisotropic turbulence on the long-term beam spread and scintillation index using the classical Kolmogorov power-law exponent $\alpha = 11/3$. In this paper, we show a quantitative analysis of the anisotropic turbulence by using a non-Kolmogorov power spectrum with an anisotropic coefficient. The spectrum used here is based on the spectrum shown in [19]; it does not include the inner and outer scales, and it is valid only inside the inertial subrange. Using this non-Kolmogorov spectrum, in weak turbulence conditions, we analyze the impact of exponent variations α on long-term beam spread and scintillation index for several anisotropic coefficient values ς. We consider only propagation across the turbulence cells where circular symmetry is maintained on the orthogonal plane to the propagation direction. In other words, we suppose that the anisotropic turbulence cells are a solid generated by the rotation of an ellipse around its semiminor axis, which is overlapped with the horizontal propagation direction. This hypothesis is essential to maintain the symmetry assumptions reported in [20] used to calculate turbulence statistics parameters, such as scintillation index. Although this hypothesis is quite strong, it should be considered as a first step toward a better understanding of a very complex problem such as anisotropic turbulence. Finally, let us note that often is more appropriate, in the context of concrete atmospheric problems, to consider anisotropic propagation along the vertical direction. In such a case, our results remain valid if we take into account the change of C_n^2 with altitude.

2. ANISOTROPIC NON-KOLMOGOROV SPECTRUM

Published theoretical papers [21,22] were dedicated to the interpretation of experiments on the scattering of radio waves, particularly on the nonisotropic character of turbulence scatterers. Such papers used a nonisotropic power spectrum in agreement with experimental data. Later, Kon [19] showed a qualitative study of nonisotropic turbulence by using the mentioned power spectrum. In this paper, we assume, as in [19], that for a laser beam propagating along a path exhibiting anisotropic turbulence, the structure function for the refractive-index fluctuations is given by

$$D_n(\vec{r}) = \beta \cdot C_n^2 \cdot \left(\frac{\Delta x^2 + \Delta y^2}{\varsigma} + \Delta z^2\right)^{\frac{\gamma}{2}}, \tag{1}$$

where $\vec{r}$ is a vector spatial variable, γ is the power law, which reduces to $2/3$ in the case of conventional Kolmogorov turbulence. Here, β is a constant equal to unity when $\gamma = 2/3$, but otherwise has units $m^{-\gamma+2/3}$ and ς is the anisotropic coefficient. The corresponding power-law spectrum associated with such structure function takes the form [20]

$$\Phi_n(\vec{\kappa},\alpha) = A(\alpha)\cdot \tilde{C}_n^2 \cdot \varsigma^2 \cdot [\kappa_z^2 + \varsigma(\kappa_x^2+\kappa_y^2)]^{-\frac{\alpha}{2}}, \qquad (2)$$

where $\alpha = \gamma + 3$ is the spectral index or power law, $\tilde{C}_n^2 = \beta \cdot C_n^2$ is a generalized structure parameter with units $m^{-\gamma}$, and $A(\alpha)$ is defined by

$$A(\alpha) = \frac{1}{4\pi^2}\Gamma(\alpha-1)\cos\left(\frac{\alpha\pi}{2}\right), \qquad 3<\alpha<4, \qquad (3)$$

and the symbol $\Gamma(x)$ in the last expression is the gamma function. When $\alpha = 11/3$ and $\varsigma = 1$, we find that $A(11/3) = 0.033$ and the generalized power spectrum reduces to the conventional Kolmogorov spectrum. Also, when the power law approaches the limiting value $\alpha = 3$, the function $A(\alpha)$ approaches zero. Consequently, the refractive-index power spectral density vanishes in this limiting case.

3. LONG-TERM BEAM SPREAD

It is well known that the beam spot size of a laser beam propagating in turbulence is affected from two main effects: beam spreading and beam wander. Random temperature fluctuations of the atmosphere yield random refractive-index fluctuations; therefore, a laser beam propagating through the atmosphere is randomly deviated from the direction of propagation (beam wander), and it is more affected from beam spreading than a diffraction-limited beam in absence of turbulence. Physically, the turbulence acts like many lenses of different size that randomly change the effective optical path of the beam. The combined effects of beam wander and beam spreading is called long-term beam spread, which represents the effective beam spot size, and it is used as one of the main parameters to evaluate the intensity profile along the path.

The analytical form of long-term beam spread for a Gaussian beam is [20]

$$W_e^2 = W_{LT}^2(\alpha) = W^2\cdot[1+T(\alpha)], \qquad (4)$$

where W is the diffraction-limited spot size radius, and $T(\alpha)$ is the term that includes small-scale beam spreading and beam wander atmospheric effects [20].

If we consider that circular symmetry is maintained on the orthogonal plane to the propagation direction, we can use the same procedure as reported in [20], but using the power spectrum Eq. (2). We carry out

$$\begin{aligned} T(\alpha) &= 4\pi^2k^2L\cdot\left(\int_0^1\int_0^\infty \kappa\cdot\phi_n(\alpha,\kappa)\mathrm{d}\kappa\mathrm{d}\xi \right.\\ &\quad \left. -\int_0^1\int_0^\infty \kappa\cdot\phi_n(\alpha,\kappa)\exp\left(-\frac{\Lambda L\kappa^2\xi^2}{k}\right)\mathrm{d}\kappa\mathrm{d}\xi\right)\\ &= 0.25\cdot\frac{\alpha}{\alpha-1}\cdot\left[\sin\left(\alpha\cdot\frac{\pi}{4}\right)\right]^{-1}\cdot\tilde{\sigma}_R^2(\alpha)\cdot\Lambda^{\frac{\alpha}{2}-1}\cdot\varsigma^{2-\alpha}\\ &= T(\alpha)_{\text{isotropic}}\cdot\varsigma^{2-\alpha}, \end{aligned} \qquad (5)$$

where $\xi = 1-\frac{z}{L}$, z is the propagation distance, L is the path length, $\Lambda = \frac{2L}{kW^2}$ $k = \frac{2\pi}{\lambda}$, $\phi_n(\alpha,\kappa)$ is the non-Kolmogorov spectrum Eq. (2), and we have defined a non-Kolmogorov Rytov variance as the plane wave scintillation index in non-Kolmogorov turbulence [23]:

$$\tilde{\sigma}_R^2(\alpha) = -8\pi^2\cdot A(\alpha)\cdot\frac{1}{\alpha}\cdot\Gamma\left(1-\frac{\alpha}{2}\right)\cdot\sin\left(\alpha\cdot\frac{\pi}{4}\right)\cdot\tilde{C}_n^2\cdot k^{3-\frac{\alpha}{2}}\cdot L^{\frac{\alpha}{2}}. \qquad (6)$$

Note that, for $\alpha = 11/3$ and $\varsigma = 1$, we obtain the particular case of the Kolmogorov spectrum already shown in [1]. Also, for $\varsigma = 1$, Eq. (5) reduces to isotropic expression shown in [1].

Then, we plot in Fig. 1 the long-term beam spread as a function of alpha for several ς setting the following parameters (W_0 is the beam spot radius): $L = 50000\,\mathrm{m}$, $\tilde{C}_n^2 = 7\cdot10^{-18}\,\mathrm{m}^{-\alpha+3}$, $\lambda = 1.55\,\mu\mathrm{m}$, and $W_0 = 0.01\,\mathrm{m}$. The value of $\tilde{C}_n^2$ has been chosen to simulate a high-altitude path, where anisotropic turbulence may be present.

We deduce from Fig. 1 that the anisotropic parameter ς influences the long-term beam spread, which is reduced if ς assume high values. Also, we deduce from Fig. 1 that alpha variations have less impact on long-term beam spread for high ς values. These deductions can be physically explained by mentioning the change of curvature of the anisotropic turbulence cells with respect to the isotropic case. Anisotropic cells change the focusing properties of the turbulence; in particular, a beam propagating along the short axis of the anisotropic cells (z direction) will be less deviated from the direction of propagation because these cells act as lenses with a higher radius of curvature. Accordingly, the long-term beam spread will be reduced, and, for high values of ς, this anisotropic effect dominates on the power-law variations.

We cannot deduce from this analysis how much impact anisotropy has on long-term beam spread with respect the inner and outer scales, which are not included in the spectrum Eq. (2); however, that could be an interesting future task.

4. SCINTILLATION INDEX

A laser beam propagating in turbulence is affected from another main effect: the scintillation. The scintillation index is denoted by

$$\sigma_I^2 = \frac{\langle I^2\rangle}{\langle I\rangle^2} - 1, \qquad (7)$$

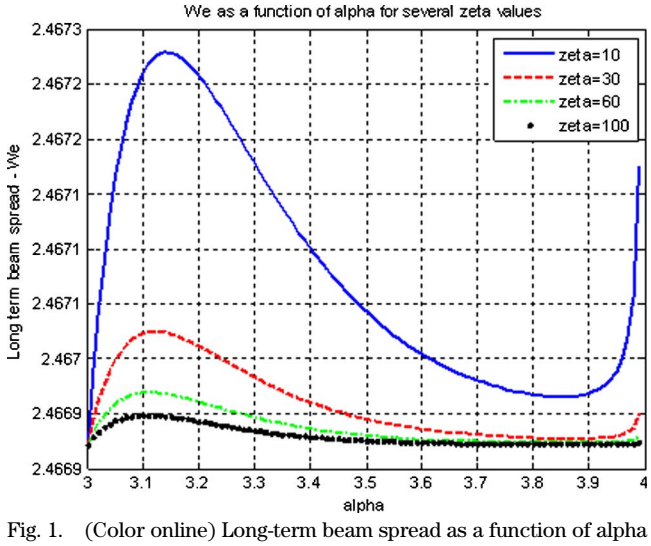

Fig. 1. (Color online) Long-term beam spread as a function of alpha for a horizontal path.

where I is the optical field irradiance and the brackets denote an ensemble, or long spatial distance, average.

In our analysis, as reported in [22], we include aperture averaging effects of the receiver aperture of diameter D_G, so we carry out the flux variance in the plane of the detector at a short distance L_f behind the collecting lens. We illustrate such a system in Fig. 2.

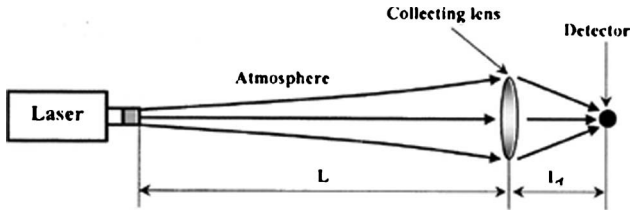

Fig. 2. Propagation geometry for a laser beam originating at distance L to the left of a thin Gaussian lens.

A. PLANE WAVE MODEL

The procedure adopted in this paper is the same as discussed in [20] for the standard Kolmogorov spectrum, but here we use a non-Kolmogorov anisotropic spectrum Eq. (2). Our analysis for the plane wave model leads to

$$\begin{aligned}\sigma_{I\text{plane}}^2(\alpha, D_G) &= 8\pi^2 \cdot k^2 \cdot L \cdot \mathrm{Re}\left\{\int_0^1 \int_0^\infty \kappa \cdot \Phi_n(\kappa, \alpha) \cdot \exp\left(-\frac{D_G^2 \cdot \kappa^2}{16}\right) \cdot \left[1 - \exp\left(-j\frac{L \cdot \kappa^2 \cdot \xi}{k}\right)\right] \mathrm{d}\kappa \mathrm{d}\xi\right\} \\ &= 8\pi^2 \cdot A(\alpha) \cdot \tilde{C}_n^2 \cdot k^{3-\frac{\alpha}{2}} \cdot L^{\frac{\alpha}{2}} \cdot \Gamma\left(1 - \frac{\alpha}{2}\right) \cdot \frac{1}{\alpha} \cdot \varsigma^{2-\alpha} \cdot \left\{\frac{\alpha}{2} \cdot \left(\frac{k \cdot D_G^2}{16 \cdot L}\right)^{\frac{\alpha}{2}-1} - \left[\left(\frac{k \cdot D_G^2}{16 \cdot L}\right)^2 + 1\right]^{\frac{\alpha}{4}} \cdot \sin\left[\frac{\alpha}{2} \cdot \mathrm{arctg}\left(\frac{16 \cdot L}{k \cdot D_G^2}\right)\right]\right\} \\ &= -\tilde{\sigma}_R^2(\alpha) \cdot \left[\sin\left(\alpha \cdot \frac{\pi}{4}\right)\right]^{-1} \cdot \varsigma^{2-\alpha} \cdot \left\{\frac{\alpha}{2} \cdot \left(\frac{k \cdot D_G^2}{16 \cdot L}\right)^{\frac{\alpha}{2}-1} - \left[\left(\frac{k \cdot D_G^2}{16 \cdot L}\right)^2 + 1\right]^{\frac{\alpha}{4}} \cdot \sin\left[\frac{\alpha}{2} \cdot \mathrm{arctg}\left(\frac{16 \cdot L}{k \cdot D_G^2}\right)\right]\right\} \\ &= \sigma_{I\text{plane}}^2(\alpha, D_G)_{\text{isotropic}} \cdot \varsigma^{2-\alpha}. \end{aligned} \tag{8a}$$

Note that if we consider a point receiver ($D_G = 0$) no aperture averaging is present and $\sigma_{I\,\text{plane}}^2(\alpha, D_G) = \tilde{\sigma}_R^2(\alpha)$, which is the non-Kolmogorov Rytov variance [Eq. (6)]. Also, for $\varsigma = 1$, Eq. (8a) reduces to the isotropic expression shown in [1].

We plot in Fig. 3 $\sigma_{I\text{plane}}^2(\alpha, D_G)$ as a function of alpha for several ς for a particular high-altitude horizontal path. We use the following set of parameters:

$$L = 50000\,\text{m}; \qquad \tilde{C}_n^2 = 7 \cdot 10^{-18}\,\text{m}^{-\alpha+3};$$
$$\lambda = 1.55\,\mu\text{m}; \qquad D_G = 0.1\,\text{m}.$$

B. SPHERICAL WAVE MODEL

Similar to the plane wave model case, the scintillation analysis for the spherical wave model leads to

$$\begin{aligned}\sigma_{I\text{spherical}}^2(\alpha, D_G) &= 8\pi^2 \cdot k^2 \cdot L \cdot \mathrm{Re}\left\{\int_0^1 \int_0^\infty \kappa \cdot \Phi_n(\kappa, \alpha) \cdot \exp\left(-\frac{D_G^2 \cdot \kappa^2 \cdot \xi^2}{16}\right) \cdot \left[1 - \exp\left(-j\frac{L \cdot \kappa^2 \cdot \xi \cdot (1-\xi)}{k}\right)\right] \mathrm{d}\kappa \mathrm{d}\xi\right\} \\ &= 4\pi^2 \cdot k^2 \cdot L \cdot A(\alpha) \cdot \tilde{C}_n^2 \cdot \left(\frac{16}{D_G^2}\right)^{1-\frac{\alpha}{2}} \cdot \Gamma\left(1 - \frac{\alpha}{2}\right) \cdot \varsigma^{2-\alpha} \cdot \left\{\frac{1}{\alpha - 1}\right. \\ &\quad \left. - \mathrm{Re}\left\{\left(j\frac{16L}{kD_G^2}\right)^{\frac{\alpha}{2}-1} \cdot \frac{2}{\alpha} \cdot {}_2F_1\left(1 - \frac{\alpha}{2}, \frac{\alpha}{2}; 1 + \frac{\alpha}{2}; 1 + j\frac{kD_G^2}{16L}\right)\right\}\right\} \\ &= \sigma_{I\text{spherical}}^2(\alpha, D_G)_{\text{isotropic}} \cdot \varsigma^{2-\alpha}, \end{aligned} \tag{8b}$$

where ${}_2F_1(a, b; c; z)$ is the hypergeometric function that is given by

$${}_2F_1(a, b; c; z) = \sum_0^\infty \frac{(a)_n \cdot (b)_n}{(c)_n} \cdot \frac{z^n}{n!}, \qquad |z| < \infty, \tag{9}$$

where

$$(a)_n = \frac{\Gamma(a + n)}{\Gamma(a)}. \tag{10}$$

We plot in Fig. 4 $\sigma_{I\text{spherical}}^2(\alpha, D_G)$ as a function of alpha for several ς for a particular high-altitude horizontal path, taking the same set of parameters as the plane wave case.

C. GAUSSIAN BEAM WAVE MODEL

To describe the beam characteristics at the input plane and the front plane of the Gaussian lens, we use two sets of non-dimensional beam parameters. We assume the transmitted Gaussian beam at the input plane has finite radius W_0 and phase front radius of curvature given by F_0. Thus, we have

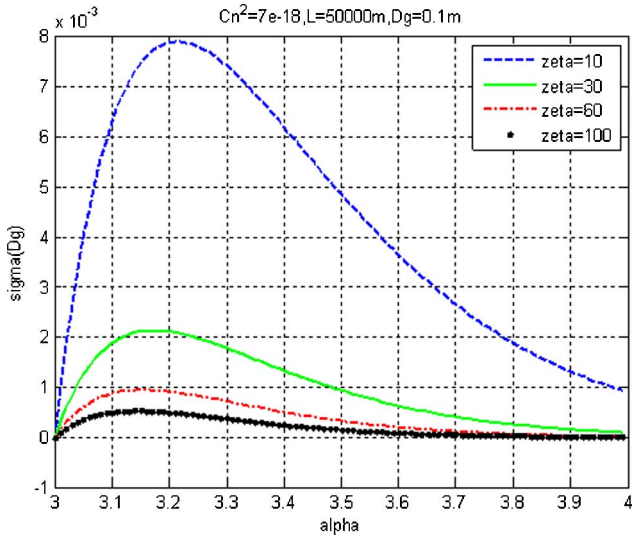

Fig. 3. (Color online) Scintillation index for the plane wave as a function of alpha for several anisotropic coefficient values.

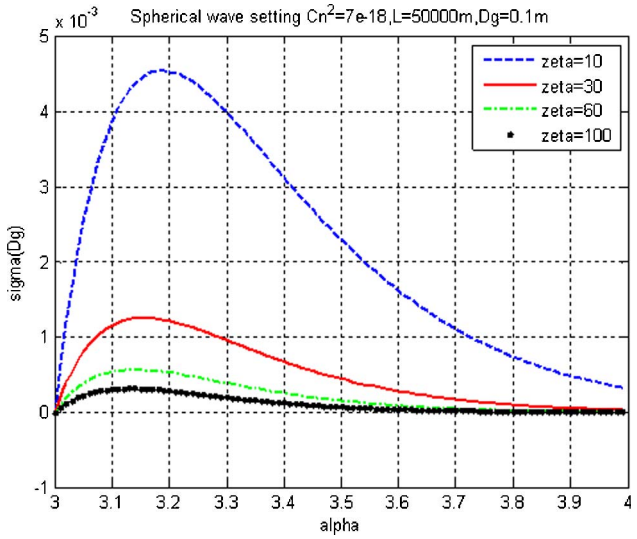

Fig. 4. (Color online) Scintillation index for the spherical wave as a function of alpha for several anisotropic coefficient values.

$$\text{at the transmitter } (z=0): \Theta_0 = 1 - \frac{L}{F_0}, \qquad \Lambda_0 = \frac{2L}{kW_0^2}, \quad (11)$$

$$\text{at the Gaussian lens } (z=L): \Theta_1 = \frac{\Theta_0}{\Theta_0^2+\Lambda_0^2}, \qquad \Lambda_1 = \frac{\Lambda_0}{\Theta_0^2+\Lambda_0^2}. \quad (12)$$

Following the same procedure discussed in [1] for the standard Kolmogorov spectrum, but here using the non-Kolmogorov anisotropic spectrum Eq. (2), our analysis for a Gaussian beam leads to (neglecting beam wander effects)

$$\begin{aligned}
&\sigma^2_{I\text{Gaussian}}(\alpha, D_G)\\
&\quad = 4\pi^2 \cdot k^{3-\frac{\alpha}{2}} \cdot L \cdot \times \mathrm{Re}\int_0^1 \int_0^\infty \kappa \cdot \Phi_n(\kappa,\alpha)\\
&\quad \cdot \exp\left\{-\frac{L\cdot\kappa^2}{k(\Lambda_1+\Omega_G)} \cdot [(1-\bar{\Theta}_1\xi)^2 + \Lambda_1\Omega_G\xi^2]\right\}\\
&\quad \cdot \left\{1 - \exp\left[-j\frac{L\kappa^2}{k}\left(\frac{\Omega_G-\Lambda_1}{\Lambda_1+\Omega_G}\right)\xi(1-\bar{\Theta}_1\xi)\right]\right\} \mathrm{d}\kappa \mathrm{d}\xi\\
&\quad = 4\pi^2 \cdot k^2 \cdot L \cdot A(\alpha) \cdot \tilde{C}_n^2 \cdot \Gamma\left(1-\frac{\alpha}{2}\right)\\
&\quad \cdot \left[\frac{k}{L}\cdot(\Lambda_1+\Omega_G)\right]^{1-\frac{\alpha}{2}} \cdot \varsigma^{2-\alpha}\\
&\quad \cdot \left\{\int_0^1 [(1-\bar{\Theta}_1\cdot\xi)^2 + \Lambda_1\Omega_G\xi^2]^{\frac{\alpha}{2}-1}\mathrm{d}\xi\right.\\
&\quad -\mathrm{Re}\int_0^1 [(1-\bar{\Theta}_1\cdot\xi)^2 + \Lambda_1\Omega_G\xi^2 + j(\Omega_G-\Lambda_1)\\
&\quad \left.\cdot\xi(1-\bar{\Theta}_1\cdot\xi)]^{\frac{\alpha}{2}-1}\mathrm{d}\xi\right\}\\
&\quad = \sigma^2_{I\text{Gaussian}}(\alpha, D_G)_{\text{isotropic}} \cdot \varsigma^{2-\alpha}. \qquad (13)
\end{aligned}$$

We plot in Fig. 5 $\sigma^2_{I\text{Gaussian}}(\alpha, D_G)$ as a function of alpha for several ς for a collimated beam ($\Theta_0 = 1$), taking the same set of parameters previously used.

We deduce from Figs. 3–5 that the anisotropic coefficient influences the scintillation index. In particular, high values of the anisotropy coefficient ς decrease the scintillation index and, at the same time, reduce the impact of α variation. These deductions can be physically explained by mentioning the change of curvature of the anisotropic turbulence cells with respect to the isotropic case. Turbulence cells act as lenses with a higher radius of curvature, leading to a reduction of amplitude fluctuations and, consequently, scintillation index. As for long-term beam spread, we cannot deduce from this analysis how much impact anisotropy has on the scintillation index with respect to the inner and outer scales. For $\varsigma = 1$, Eq. (13) reduces to the isotropic expression shown in [24].

5. ANISOTROPIC FACTOR

The main result deduced from all the previously reported expressions is the multiplicative factor $\varsigma^{2-\alpha}$, which essentially introduces a turbulence rescaling due to anisotropic and non-Kolmogorov turbulence.

We plot the anisotropic factor $\varsigma^{2-\alpha}$ as a function of α for several ς values. Results are shown in Fig. 6.

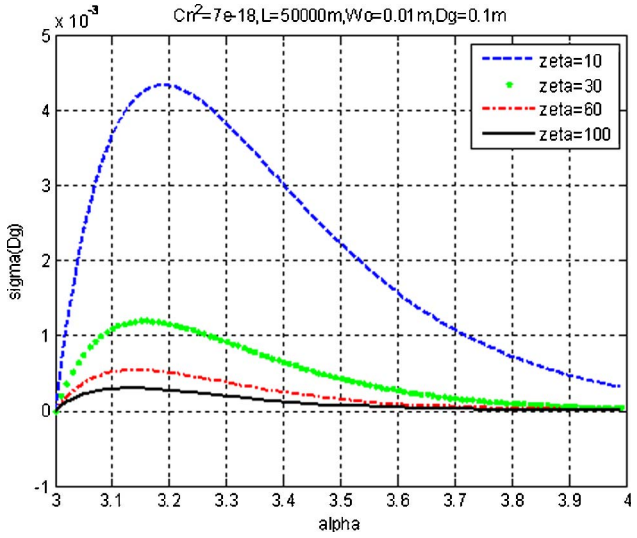

Fig. 5. (Color online) Scintillation index for the Gaussian beam as a function of alpha for several anisotropic coefficient values.

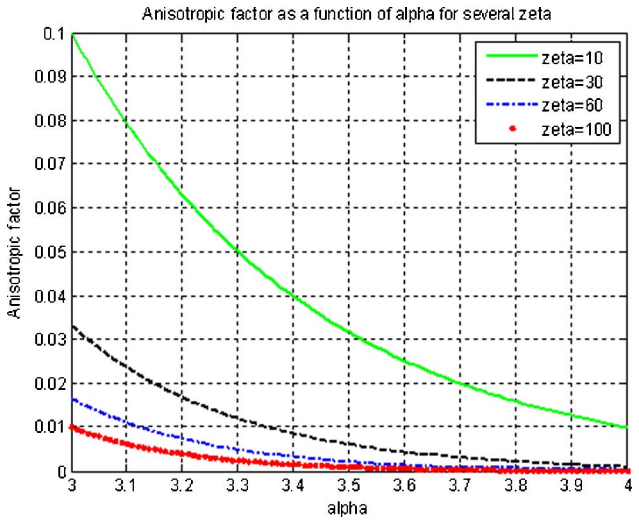

Fig. 6. (Color online) Anisotropic factor as a function of alpha for several zeta values.

We deduce from Fig. 6 that the anisotropic factor decreases as the alpha value increases for every zeta value. Also, high zeta values reduce the anisotropic factor and, consequently, the atmospheric turbulence parameters (scintillation index and long-term beam spread).

In this paper, we supposed that the anisotropic factor has the same effect on all the turbulence scales. However, in stable atmospheric boundary layers, isotropy probably prevails at small scales. Therefore, in this case, we should distinguish small scales from other scales by using a more complete power spectrum with a filter function. Finally, we cannot deduce from Fig. 6 how much the anisotropic factor is significant in practice, given all the inaccuracies in estimating structure function parameters, outer scales, etc., that occur. Future experiments will give us an idea about the validity of this theoretical model.

6. DISCUSSION

In this paper, we used a non-Kolmogorov refractive-index structure function and a non-Kolmogorov power spectrum with an anisotropic coefficient ς to describe anisotropic turbulence. We assumed that the circular symmetry is maintained on the orthogonal plane to the propagation direction z, and we analyzed, in weak turbulence condition, long-term beam spread and scintillation index for a horizontal path and for several anisotropic coefficient values ς. We concluded that the anisotropic parameter influences both the long-term beam spread and the scintillation index by the factor $\varsigma^{2-\alpha}$. Therefore, a high value of ς decreases both the long-term beam spread and the scintillation index. Finally, we showed that power-law α variations have less impact on both the long-term beam spread and the scintillation index as ς increase.

These conclusions can be physically explained by mentioning the change of curvature of the anisotropic turbulence cells with respect to the isotropic case. Anisotropic cells change the focusing properties of the turbulence; in particular, a laser beam propagating along the short axis of the cells (z direction) will be less deviated from the direction of propagation because these cells act as lenses with a higher radius of curvature. Accordingly, the long-term beam spread will be reduced, and, for high values of ς, this anisotropic effect dominates on the α variations. For the same reason, amplitude fluctuations decrease as compared with the isotropic case, leading to a reduction of the scintillation index.

Unfortunately, we cannot deduce from this analysis how much impact anisotropy has on both the long-term beam spread and the scintillation index with respect the inner and outer scales. Also, we supposed that the anisotropic factor has the same effect on all the turbulence scales; however, in stable atmospheric boundary layers, isotropy probably prevails at small scales. Therefore, in this case, we should distinguish small scales from other scales by using a more complete power spectrum, which should include also a filter function. Finally, we are aware that this anisotropic turbulence spectrum needs to be validated by comparing theoretical results with experimental data. Therefore, this paper should be considered the first step of a more complete analysis that should be based on new experiments.

ACKNOWLEDGMENTS

This research was performed while the author I. Toselli held a National Research Council Research Associateship Award at Spacecraft Research and Design Center, Department of Mechanical and Astronautical Engineering, Naval Postgraduate School, Monterey, California.

REFERENCES

1. I. Toselli, L. C. Andrews, and R. L. Phillips, "Free space optical system performance for laser beam propagation through non-Kolmogorov turbulence," Opt. Eng. **47**, 026003 (2008).
2. D. Dayton, B. Pierson, and B. Spielbusch, "Atmospheric structure function measurements with a Shack-Hartmann wave front sensor," Opt. Lett. **17**, 1737–1739 (1992).
3. A. Tunik, "Analysis of free-space laser signal intensity over a 2.33 km optical path," Proc. SPIE **6708**, 670802 (2007).
4. M. S. Be1enkii, S. J. Karis, J. M. Brown II, and R. Q. Fugate, "Experimental study of the effect of non-Kolmogorov stratospheric turbulence on star image motion," Proc. SPIE **3126**, 113–123 (1997).
5. B. E. Stribling, B. M. Welsh, and M. C. Roggemann, "Optical propagation in non-Kolmogorov atmospheric turbulence," Proc. SPIE **2471**, 181–196 (1995).
6. D. T. Kyrazis, J. Wissler, D. D. B. Keating, A. J. Preble, and K. P. Bishop, "Measurement of optical turbulence in the upper troposphere and lower stratosphere," Proc. SPIE **2120**, 43–55 (1994).
7. C. I. Moore, H. R. Burris, W. S. Rabinovich, L. Wasiczko, M. R. Suite, L. A. Swingen, R. Mahon, M. F. Stell, G. C. Gilbreath, and W. J. Scharpf, "Overview of NRL's maritime laser communication test facility," Proc. SPIE **5892**, 589206 (2005).
8. L. M. Wasiczko, C. I. Moore, H. R. Burris, M. Suite, M. Stell, and W. Rabinovich, "Studies of atmospheric propagation in the maritime environment at NRL," Proc. SPIE **6551**, 65510F (2007).
9. L. M. Wasiczko, R. Mahon, C. I. Moore, H. R. Burris, M. Suite, and W. Rabinovich, "Power spectra of a free space optical link in a maritime environment," Proc. SPIE **7464**, 746407 (2009).
10. M. Chang, C. O. Font, F. Santiago, Y. Luna, E. Roura, and S. Restaino, "Marine environment optical propagation measurements," Proc. SPIE **5550**, 40–46 (2004).
11. F. S. Vetelino, K. Grayshan, and C. Y. Young, "Inferring path average Cn^2 values in the marine environment," J. Opt. Soc. Am. A **24**, 3198–3206 (2007).
12. A. S. Gurvich and M. S. Belen'kii, "Influence of stratospheric turbulence on infrared imaging," J. Opt. Soc. Am. A **12**, 2517–2522 (1995).
13. M. S. Belen'kii, "Effect of the stratosphere on star image motion," Opt. Lett. **20**, 1359–1361 (1995).

14. M. S. Belen'kii, J. D. Barchers, S. J. Karis, C. L. Osmon, J. M. Brown II, and R. Q. Fugate, "Preliminary experimental evidence of anisotropy of turbulence and the effect of non-Kolmogorov turbulence on wavefront tilt statistics," Proc. SPIE **3762**, 396–406 (1999).
15. M. S. Belen'kii, E. Cuellar, K. A. Hughes, and V. A. Rye, "Experimental study of spatial structure of turbulence at Maui Space Surveillance Site (MSSS)," Proc. SPIE **6304**, 63040U (2006).
16. M. S. Belen'kii, S. J. Karis, and C. L. Osmon, "Experimental evidence of the effects of non-Kolmogorov turbulence and anisotropy of turbulence," Proc. SPIE **3749**, 50–51 (1999).
17. R. R. Beland, "Some aspects of propagation through weak isotropic non-Kolmogorov turbulence," Proc. SPIE **2375**, 6–16 (1995).
18. L. J. Hotten, L. C. Roggemann, B. A. Jones, J. Lane, and D. G. Black, "High bandwidth atmospheric turbulence data collection platform," Proc. SPIE **3866**, 23–32 (1999).
19. A. I. Kon, "Qualitative theory of amplitude and phase fluctuations in a medium with anisotropic turbulent irregularitie," Waves Rand. Compl. Media **4**, 297–305 (1994).
20. L. C. Andrews and R. L. Phillips, *Laser Beam Propagation through Random Media*, 2nd ed. (SPIE, 2005).
21. A. S. Gurvich and A. I. Kon, "The backscattering from anisotropic turbulent irregularities," J. Electromagn. Waves Appl. **6**, 107–118 (1992).
22. A. S. Gurvich and A. I. Kon, "Aspect sensitivity of radar returns from anisotropic turbulent irregularities," J. Electromagn. Waves Appl. **7**, 1343–1353 (1993).
23. I. Toselli, L. C. Andrews, R. L. Phillips, and V. Ferrero, "Scintillation index of optical plane wave propagating through non Kolmogorov moderate-strong turbulence," Proc. SPIE **6747**, 67470B (2007).
24. I. Toselli, L. C. Andrews, R. L. Phillips, and V. Ferrero, "Free space optical system performance for a Gaussian beam propagating through non-Kolmogorov turbulence," IEEE Trans. Antennas Propag. **57**, 1783–1788 (2009).